

NON-LINEAR FINITE ELEMENT ANALYSIS OF DYNAMICALLY LOADED STRUCTURES

Á. KOVÁCS

Department of Technical Mechanics
Technical University, H-1521 Budapest

Received November 10, 1987
Presented by Prof. Dr. Gy. Béda

Abstract

An effective finite element method has been presented for calculating transient response of dynamically loaded structures. The so-called implicit-explicit algorithm is suitable to analyse geometrically and materially non-linear problems. The analytic integration of Prager's kinematic hardening rule permits the 'exact' calculation of stresses during plastic deformation.

Introduction

In the last two decades significant advances have been made in the development and application of numerical methods to the solution of dynamic problems. This paper presents an application of the so-called implicit-explicit algorithm to the solution of geometrically and materially non-linear dynamic problems. Dynamic loads can be caused due to impact, explosions and earthquakes which are of considerable importance in the safety studies of nuclear reactors in hypothetical accidents, automotive and aircraft phenomena, and many other areas.

In most of numerical solutions of dynamic problems the equations of motion are first discretised in space. This procedure is called semidiscretisation and yields a set of ordinary differential equations in time. The semidiscretisation using finite elements has been successfully used in the determination of transient response of dynamically loaded structures. There are two basic types of methods for integrating the equations of motion: direct integration methods and modal superposition techniques.

The modal superposition technique is normally used for linear problems only.

The direct integration methods can be further subdivided into explicit and implicit methods. In explicit methods difference equations are used that permit the displacements at the next time step to be found in terms of the accelerations and displacements at the previous time step, so that the procedure does not involve the solution of any equations. In implicit methods the difference equations for the displacements at the next time step involve the accelerations at the next time step, so the determination of the displacements involves the solution of a system of equations.

For this reasons implicit algorithms usually require considerably more computational effort per time step as compared with explicit methods. On the other hand, explicit algorithms require very small time steps to ensure numerical stability, while in implicit methods the time step is only restricted by accuracy requirements.

To circumvent these difficulties, methods have been developed in which it is attempted to simultaneously achieve the attributes of both algorithms. Belytschko and Mullen [1] have presented a formulation in which the elements are partitioned into three sets: implicit, explicit and interface; and the nodes are partitioned into two sets: implicit and explicit. In each time step the order of the integration was depending on the form of coupling of the elements because of stability conditions. For linear systems Hughes and Liu [2, 3] introduced the implicit-explicit concept. In their method the elements are partitioned into implicit and explicit sets only, and there was no restriction on the order of integration. This concept was extended to non-linear problems by Hughes et al. [4]. Based on this method a finite element program has been published in [5]. This program deals with plane stress, plane strain and axisymmetric applications. Geometrically and materially non-linear behaviour was taken into account using a total Lagrangian formulation and a linear elastic-plastic isotropic hardening model. Isotropic hardening model does not include Bauschinger-effect which was experimentally observed during cycling loadings. The alternation of loadings and unloadings in the dynamic problems is similar to cycling loading, so that a kinematic hardening rule probably gives a more accurate solution. Szabó and Kovács [6] report on a subroutine which is based upon the exact integration of Prager's kinematic hardening rule presented by Xucheng and Liangming [7].

Finite element formulation

After the spatial discretisation the resulting system of equations of motion for the dynamic problem becomes at time step $t_n + \Delta t$:

$$\mathbf{M} \cdot \ddot{d}_{n+1} + P_{n+1}(d) = F_{n+1}(t) \quad (1)$$

in which d is the nodal displacement vector, \mathbf{M} is the structural mass matrix (independent of time or displacement), $F_{n+1}(t)$ are the applied or activating forces, dots

denote differentiation in time. The term P_{n+1} is the internal set of forces. For linear situations:

$$P_{n+1} = \int_V \mathbf{B}^T \cdot \sigma_{n+1} dV = \mathbf{K} \cdot d_{n+1} \quad (2)$$

where \mathbf{B} is the appropriate matrix expressing the strains in terms of nodal displacements, σ_{n+1} is the vector of the 2nd Piola—Kirchhoff stresses, \mathbf{K} is the structural stiffness matrix.

In non-linear cases P_{n+1} can be estimated as

$$P_{n+1} = P_n + \mathbf{K}_n \cdot \Delta d \quad (3)$$

$$\Delta d = d_{n+1} - d_n$$

where \mathbf{K}_n is the tangential stiffness matrix evaluated from conditions at time t_n . \mathbf{K}_n can be divided into two parts:

$$\mathbf{K}_n = \mathbf{K}_L + \mathbf{K}_{NL} \quad (4)$$

The linear stiffness matrix can be calculated as

$$\mathbf{K}_L = \int_V \mathbf{B}^T \mathbf{D}^{ep} \mathbf{B} dV \quad (5)$$

where \mathbf{D}^{ep} is the constitutive matrix.

The non-linear stiffness matrix is given as ([5])

$$\mathbf{K}_{NL} = \int_V \mathbf{G}^T \mathbf{H} \cdot \mathbf{G} dV \quad (6)$$

in which \mathbf{H} is a stress matrix formed from the stress components of σ and \mathbf{G} is a matrix including the derivatives of the shape functions.

Material nonlinearity

The constitutive equations can be written as

$$d\sigma = \mathbf{D}^{ep} d\varepsilon. \quad (7)$$

The constitutive matrix can be calculated using the Prandtl—Reuss theory. The total strain increment can be divided into elastic and plastic parts:

$$d\varepsilon = d\varepsilon^e + d\varepsilon^p. \quad (8)$$

With the elastic strain increment the Hooke-law can be written as

$$d\sigma^e = \mathbf{D}^e \cdot d\varepsilon^e \quad (9)$$

where \mathbf{D}^e is the elastic constitutive matrix.

Assuming an associated flow rule the plastic strain increment is proportional to the stress gradient of the yield function (now given by the Mises yield condition):

$$d\varepsilon^p = d\lambda \frac{\partial f}{\partial \sigma} \quad (10)$$

If $a \equiv \partial f / \partial \sigma$ then according to [5] the constitutive matrix is as follows

$$\mathbf{D}^{ep} = \mathbf{D}^e - \frac{bb^T}{H' + b^T a} \quad (11)$$

in which

$$b = \mathbf{D}^e \cdot a \quad (12)$$

and

$$H' = \frac{E_T E}{E - E_T} \quad (13)$$

(see Fig. 1).

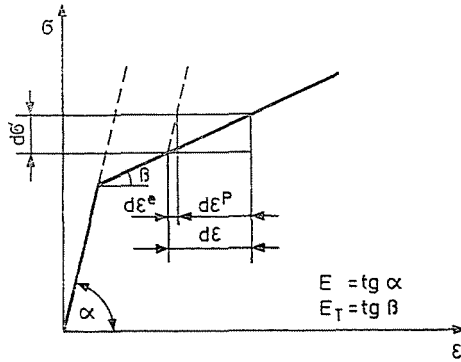


Fig. 1. Elasto-plastic strain hardening for the uniaxial case

The available methods of integrating eq. (7) are mostly numerical ones. The method proposed in [7] and applied in [6] is an exact integration for a kinematic hardening model.

Prager's kinematic hardening rule can be written as

$$\dot{S} = 2G \cdot \dot{\varepsilon}' - \frac{9G^2}{\sigma_F^2(3G + H')} a \cdot a^T \cdot \dot{\varepsilon}', \quad (14)$$

$$a = S - \alpha$$

where S is the vector of the stress deviatoric tensor, α is the vector of the translation tensor of the coordinates of the center of the yield surface, ε' is the vector of the strain deviatoric tensor, G is the shear modulus of the material, σ_F is the yield stress.

The following relation can be written for $\dot{\alpha}$ and for the plastic strain rate:

$$\dot{\alpha} = \frac{2}{3} H' \cdot \dot{\epsilon}^p = \frac{3G \cdot a^T \cdot \dot{\epsilon}'}{R_0^2(3G + H')} a \tag{15}$$

where $R_0 = \sqrt{\frac{2}{3}} \sigma_F$ denotes the radius of the yield surface in the stress deviatoric space. From eqs (14) and (15), we can obtain

$$\dot{a} = 2 \cdot G \cdot \dot{\epsilon}' - \frac{2G}{R_0^2} (a^T \cdot \dot{\epsilon}') a. \tag{16}$$

If we define β as the angle between a and $\dot{\epsilon}'$, and suppose that $\dot{\epsilon}'$ is invariable during a time step Δt , from the above equations, we can obtain a differential equation as following

$$\dot{\beta} = \frac{2G \cdot |\dot{\epsilon}'|}{R} \sin \beta. \tag{17}$$

The solution of eq. (17) in the time interval $t_i \equiv t \equiv t_{i+1}$:

$$\beta(t) = 2 \operatorname{arctg} \left(e^{-mt} \operatorname{tg} \frac{\beta_i}{2} \right), \tag{18}$$

where $m = 2G \cdot |\dot{\epsilon}'| / R_0$ and at time t_i :

$$\beta(t) = \beta_i = \text{constant}. \tag{19}$$

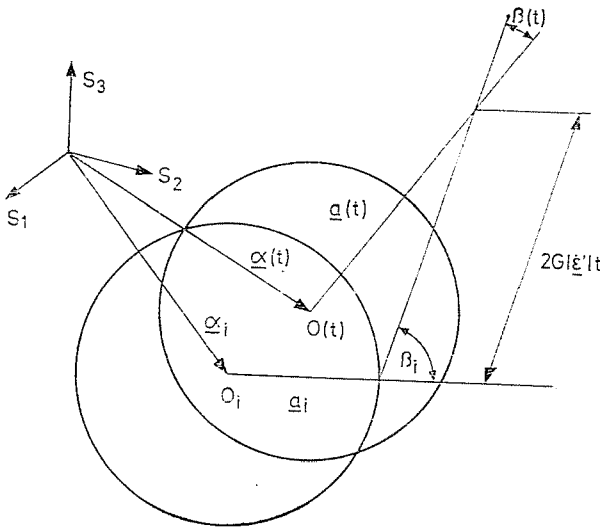


Fig. 2. Yield surfaces in the stress deviatoric space

From Fig. 2 with the aid of triangular identities we have

$$a(t) = p_1 a_i + p_2 \cdot 2G \cdot \dot{\varepsilon}' \cdot t = p_1 \left(a_i + \frac{p_2}{p_1} 2G \cdot \dot{\varepsilon}' \cdot t \right) \quad (20)$$

in which

$$p_1 = \frac{2e^{-mt}}{1 + \cos \beta_i + e^{-mt}(1 - \cos \beta_i)} \quad (21)$$

and

$$\frac{p_2}{p_1} = \frac{1}{mt} \left(\frac{\sin \beta_i}{\operatorname{tg} \beta} - \cos \beta_i \right). \quad (22)$$

From eqs (18) and (22), we obtain

$$\frac{p_2}{p_1} = \frac{1 - e^{-2mt} + (1 - e^{-mt})^2 \cos \beta_i}{2mte^{-mt}}. \quad (23)$$

From the above equations, substituting Δt for t and substituting eq. (20) into eq. (15) and integrating it, a_{i+1} and α_{i+1} can be obtained at the end of the time step or the iteration is as follows

$$\alpha_{i+1} = \alpha_i + l \cdot [(1-p) \cdot a_i + 2 \cdot b \cdot G \cdot \Delta \varepsilon'] \quad (24)$$

$$a_{i+1} = p \cdot a_i + 2 \cdot q \cdot G \cdot \Delta \varepsilon', \quad (25)$$

where

$$q = \frac{1 - e^{-2m\Delta t} + (1 - e^{-m\Delta t})^2 \cos \beta_i}{c \cdot m \cdot \Delta t}$$

$$c = 1 + \cos \beta_i + (1 - \cos \beta_i) e^{-2m\Delta t}$$

$$b = \frac{1}{m\Delta t} \left[1 + m\Delta t - \frac{2 + 2(1 - e^{-m\Delta t}) \cos \beta_i}{c} \right]$$

$$p = \frac{2e^{-m\Delta t}}{c} \quad k = m\Delta t + \ln(c/2)$$

$$l = \frac{H'}{3G + H'}$$

$$\Delta \varepsilon' = \dot{\varepsilon}' \Delta t.$$

Using eqs (24) and (25), from the known σ_i , α_i quantities at time t_i with the strain increment $\Delta \varepsilon$, the unknown σ_{i+1} , α_{i+1} quantities can be obtained as follows:

$$S_{i+1} = a_{i+1} + \alpha_{i+1} \quad (26)$$

$$\sigma_{i+1} = S_{i+1} + K \cdot (i^T \cdot \Delta \varepsilon') \cdot i + \frac{1}{3} (i^T \cdot \sigma_i) \cdot i \quad (27)$$

where

$$K = E/[3(1-2\nu)] \quad \text{and} \quad i^T = [1 \ 1 \ 0 \ 1].$$

Implicit-explicit algorithm

In the implicit-explicit method the finite element mesh contains two groups of elements: the implicit group and the explicit group. The superscripts I and E will henceforth refer to the implicit and explicit groups, respectively.

In the implicit-explicit algorithm we iterate within each time step in order to satisfy the equation of motion:

$$\mathbf{M} \cdot \ddot{\mathbf{d}}_{n+1} + P^I(d_{n+1}) + P^E(d_{n+1}) = F_{n+1}, \quad (28)$$

in which

$$\mathbf{M} = \mathbf{M}^I + \mathbf{M}^E, \quad F_{n+1} = F_{n+1}^I + F_{n+1}^E \quad \text{and}$$

$$\tilde{\mathbf{d}}_{n+1} = \mathbf{d}_{n+1}^{[0]}.$$

We assume that \mathbf{M}^E is diagonal. The algorithm is as follows ([5]):

1. step — Set iteration counter: $i=0$
2. step — Begin predictor phase in which we set:

$$\mathbf{d}_{n+1}^{[i]} = \tilde{\mathbf{d}}_{n+1} = \mathbf{d}_n + \Delta t \cdot \dot{\mathbf{d}}_n + \frac{\Delta t^2}{2} (1-2\beta) \cdot \ddot{\mathbf{d}}_n$$

$$\dot{\mathbf{d}}_{n+1}^{[i]} = \dot{\mathbf{d}}_n + \Delta t \cdot (1-\gamma) \cdot \ddot{\mathbf{d}}_n$$

$$\ddot{\mathbf{d}}_{n+1}^{[i]} = \mathbf{0}$$

3. step — Evaluate residual forces using the equation

$$\psi^{[i]} = F_{n+1} - \mathbf{M} \cdot \ddot{\mathbf{d}}_{n+1}^{[i]} - P^I(d_{n+1}) - P^E(d_{n+1})$$

4. step — If required, form the effective stiffness matrix

$$\mathbf{K}^* = \frac{1}{\Delta t^2 \beta} \mathbf{M} + \mathbf{K}_n^I$$

Otherwise use a previously calculated \mathbf{K}^* .

5. step — Solve the following system of linear equations:

$$\mathbf{K}^* \cdot \Delta \mathbf{d}_{n+1}^{[i]} = \psi_{n+1}^{[i]}$$

6. step — Enter corrector phase in which we set

$$\mathbf{d}_{n+1}^{[i+1]} = \mathbf{d}_{n+1}^{[i]} + \Delta \mathbf{d}_{n+1}^{[i]}$$

$$\ddot{\mathbf{d}}_{n+1}^{[i+1]} = \frac{1}{\Delta t^2 \beta} (\mathbf{d}_{n+1}^{[i+1]} - \mathbf{d}_{n+1}^{[i]})$$

$$\dot{\mathbf{d}}_{n+1}^{[i+1]} = \dot{\mathbf{d}}_{n+1}^{[i]} + \Delta t \cdot \gamma \cdot \ddot{\mathbf{d}}_{n+1}^{[i]}$$

7. step — Check convergence:

$$\frac{\| \Delta d_{n+1}^{[i]} \|}{\| d_{n+1}^{[i+1]} \|} \stackrel{?}{<} \varepsilon \begin{cases} \text{yes: } \rightarrow 8. \text{ step} \\ \text{no: } i = i + 1 \rightarrow 3. \text{ step} \end{cases}$$

8. step — Set

$$d_{n+1} = d_{n+1}^{[i+1]}$$

$$\dot{d}_{n+1} = \dot{d}_{n+1}^{[i+1]}$$

$$\ddot{d}_{n+1} = \ddot{d}_{n+1}^{[i+1]}$$

for use in the next time step. Set $n = n + 1$, form P and begin the next time step.

Stability analysis

The implicit-explicit algorithm include three free parameters: β , γ and Δt . Their values govern the accuracy and stability of the algorithm. Hughes and Liu [2] and Key [8] have discussed the stability limits for this scheme.

Unconditional stability of the implicit group is achieved with

$$\gamma \cong \frac{1}{2} \quad \text{and} \quad \beta = \frac{\left(\gamma + \frac{1}{2} \right)^2}{4}. \quad (29)$$

The time step is then restricted by the explicit element group. The maximum stable time step is determined from

$$\Delta t_{\text{crit}} \cong \frac{2}{\omega_{\text{max}}}, \quad (30)$$

where ω_{max} is the maximum frequency of the explicit group. We can estimate ω_{max} as

$$\omega_{\text{max}} \cong \max_{(e)} (\omega_{\text{max}}^{(e)}), \quad (31)$$

where $\omega_{\text{max}}^{(e)}$ is the maximum frequency of the e -th element of the explicit group. If only implicit elements are used and the (29) conditions are satisfied, then for reasonable accuracy the time step should be limited to ([9]):

$$\Delta t < 0.01 T_{\text{max}} \quad (32)$$

where T_{max} is the largest period. We can obtain T_{max} and ω_{max} from the solution of the generalised eigenvalue-eigenvector problem:

$$\mathbf{K} \cdot \varphi = \omega^2 \mathbf{M} \cdot \varphi \quad (33)$$

and the inverse problem

$$\mathbf{M} \cdot \ddot{\varphi} = \frac{1}{\omega^2} \mathbf{K} \cdot \varphi \tag{34}$$

respectively. Using the Stodola-iteration (Rayleigh-quotient) method we can find the largest period from eq. (33) with

$$T_{\max} = \frac{2\pi}{\omega_{\min}} \tag{35}$$

and ω_{\max} from eq. (34) with

$$\omega_{\max} = \left(\frac{1}{\omega} \right)_{\min} . \tag{36}$$

Implementation

To implement the above formulation the program TRADYN was employed which is based on program MIXDYN [5]. The program TRADYN is available for elastic-plastic kinematic hardening analysis with total Lagrangian description by using plane stress, plane strain or axisymmetric elements. Combined geometrical and material nonlinear problems can also be analysed.

Elastic large displacements of a cantilever [10, 11, 12]

The cantilever in Fig. 3 was analysed for a uniformly distributed load using five 8-node plane stress isoparametric elements. The material of the cantilever was assumed to be isotropic and linear elastic. According to beam theory, the static small deflection is $w=90,5$ [mm]. To calculate the large deflection we used the analytical solution given by Holden [13]. It was $w=82.8$ [mm]. The linear transient response

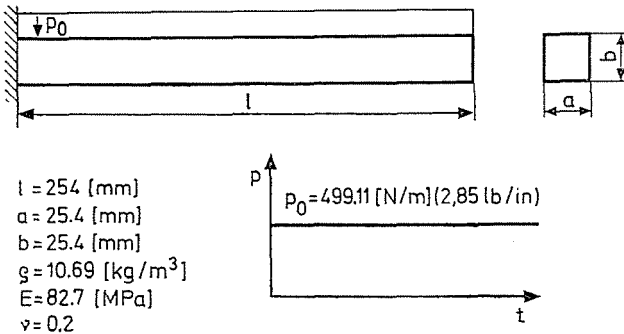


Fig. 3. Uniformly loaded cantilever

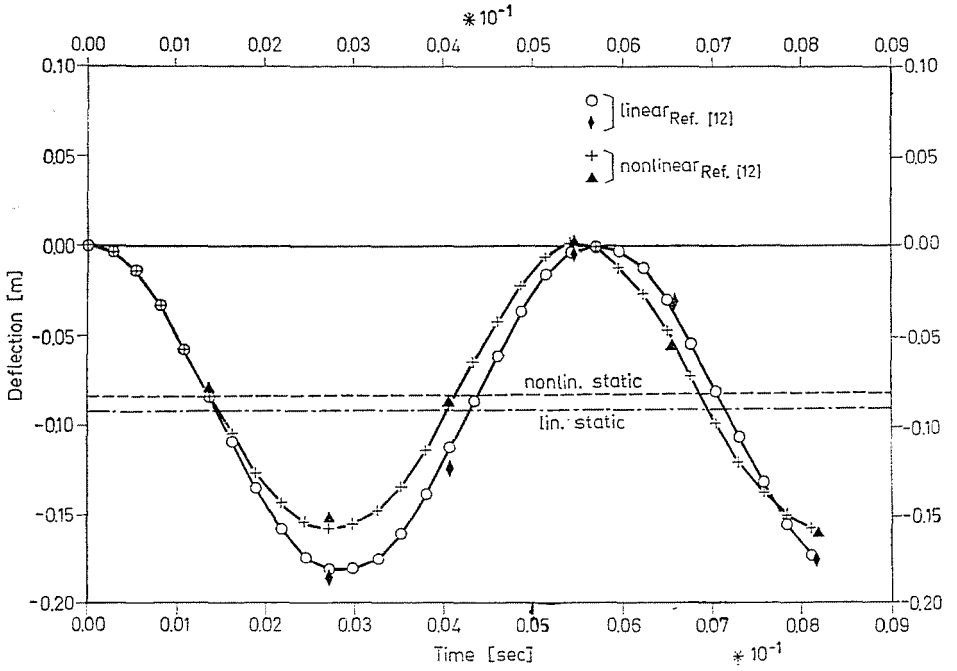


Fig. 4. Linear and non-linear transient response of the cantilever

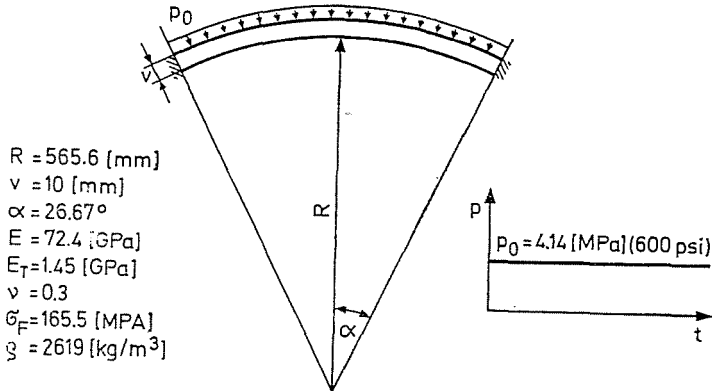


Fig. 5. Spherical shell cap submitted to step pressure loading

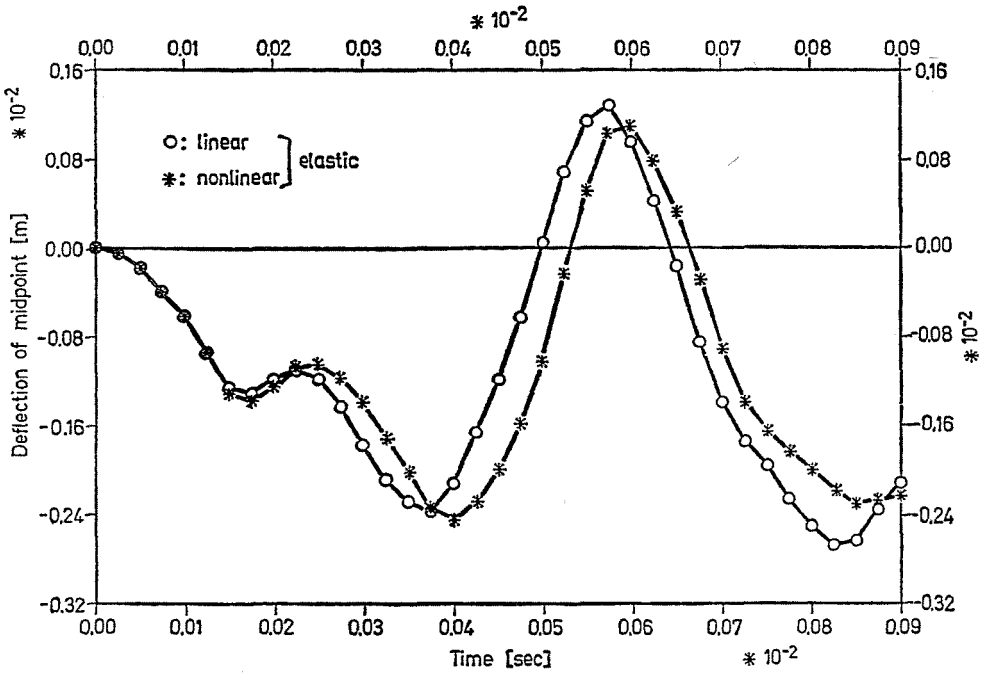


Fig. 6. Comparison of elastic transient responses of the spherical shell cap

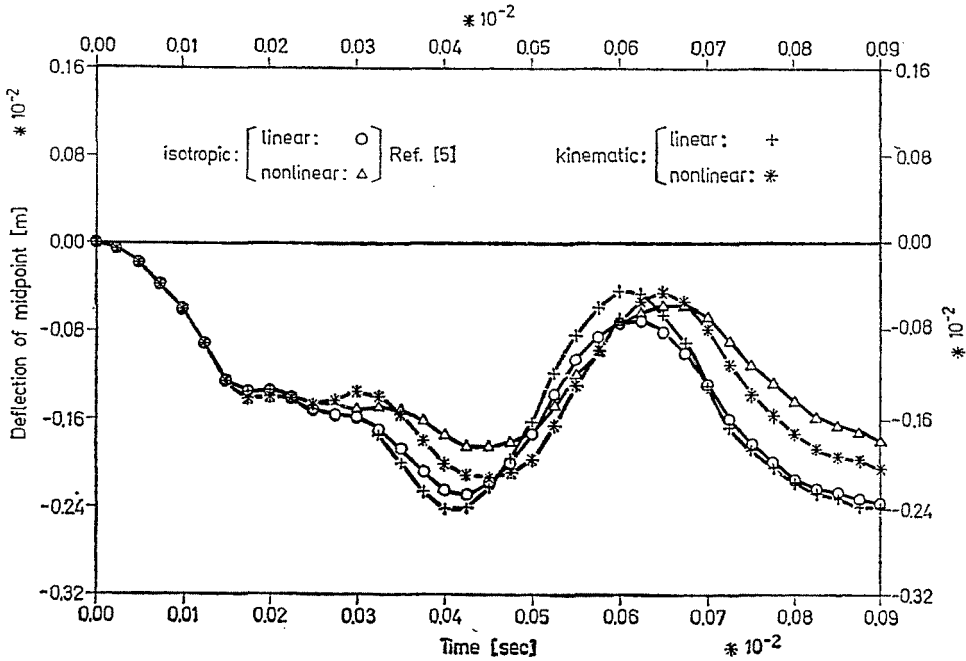


Fig. 7. Comparison of materially nonlinear transient responses of the spherical shell cap

was determined by using the Laplace-transformation. Figure 4 shows the comparison between linear and non-linear responses. The non-linear analysis was carried out using a time step $\Delta t \approx T_{\max}/21 = 2,7 \cdot 10^{-4}$ [s]. The stiffening of the cantilever in the non-linear case markedly damps out the amplitude and shortens the period of oscillations.

Elastic-plastic analysis of a spherical shell cap [5, 14, 15, 16, 17]

Ten axisymmetric elements are used to make the finite element model of the spherical shell cap shown in Figs 5, 6 and 7 show the vertical displacement at mid point using materially linear and non-linear model. It is seen from the Figures that material and geometric non-linear effects are very significant. The amplitude decay and period elongation is due to plastic deformation. In the reference solutions

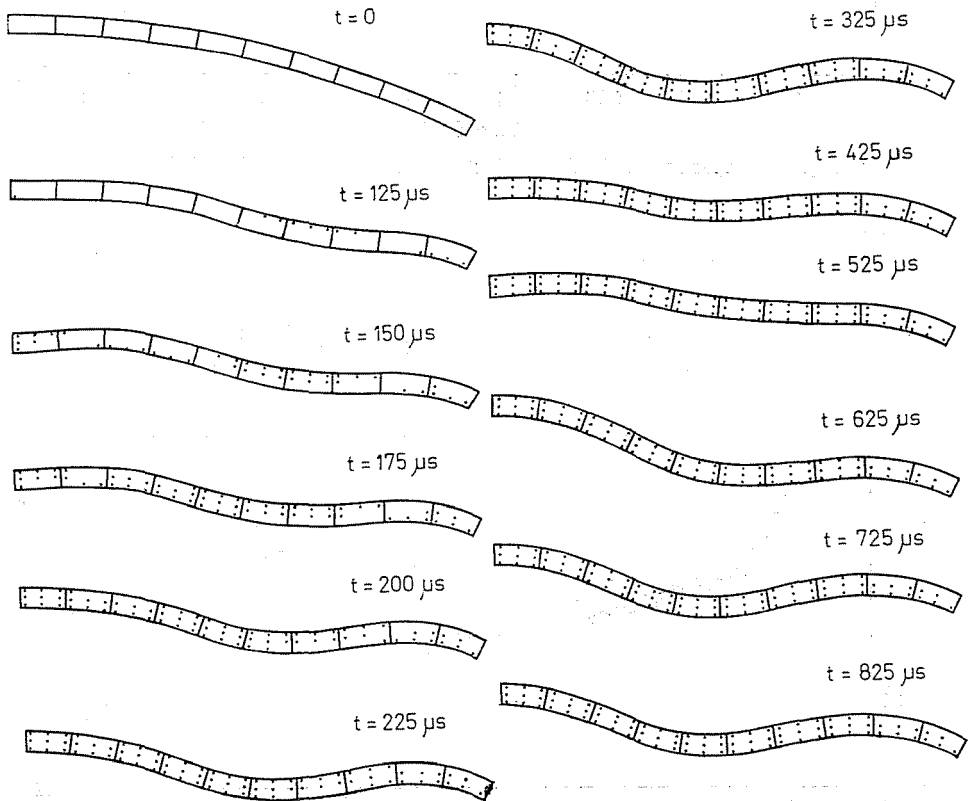


Fig. 8: Deformed shapes of the spherical shell cap with plastic zones

isotropic hardening was used. In linear analysis kinematic hardening does not modify the response as in the non-linear case.

Assuming large displacements, with the use of kinematic hardening the deformed shapes with the instantaneous plastic zones in some moments are shown in Fig. 8.

References

1. BELYTSCHKO, T., MULLEN, R.: Mesh partitions of explicit-implicit time integration, U.S. — Germany Symp. on Formulations and Comp. Algorithms in FE Analysis, MIT, Cambridge, MA, Aug. (1976).
2. HUGHES, T. J. R., LIU, W. K.: Implicit-explicit finite elements in transient analysis: implementation and numerical examples, *J. Appl. Mech. ASME*, *45*, 375—378 (1978).
3. HUGHES, T. J. R., LIU, W. K.: Implicit-explicit finite elements in transient analysis: stability theory, *J. Appl. Mech. ASME*, *45*, 371—374 (1978).
4. HUGHES, T. J. R., PISTER, K. S., TAYLOR, R. L.: Implicit-explicit finite elements in nonlinear transient analysis, *Comp. Meth. Appl. Mech. Engng*, *17/18*, 159—182 (1979).
5. OWEN, D. R. J., HINTON, E.: *Finite Elements in Plasticity. Theory and Practice*, Pineridge Press Ltd. Swansea U.K. (1980).
6. SZABÓ L., KOVÁCS Á.: Numerical implementation of Prager's kinematic hardening model in exactly integrated form for elasto-plastic analysis, *Computers & Structures*, *26*, 815—822 (1987).
7. XUCHENG, W., LIANGMING, C.: Exact integration of constitutive equations of kinematic hardening material and its extended applications, *SMiRT 8*, L2/3, 65—70 (1985).
8. KEY, S. W.: Transient response by time integration: review of implicit and explicit operators, 71—95 in Donéa, J.: *Advanced Structural Dynamics*, Applied Science Publishers Ltd. London (1980).
9. WILSON, E. L., FARHOOMAND, I., BATHE, K. J.: Nonlinear dynamic analysis of complex structures, *Earthquake Engineering and Structural Dynamics*, *1*, 241—252 (1973).
10. SHANTARAM, D., OWEN, D. R. J., ZIENKIEWICH, O. C.: Dynamic transient behavior of two- and three-dimensional structures including plasticity, large deformation effects and fluid interaction, *Earthquake Engineering and Structural Dynamics*, *4*, 561—578 (1976).
11. BATHE, K. J., RAMM, E., WILSON, E. L.: Finite element formulations for large deformation dynamic analysis, *Int. J. Num. Meth. Engng*, *9*, 353—386 (1975).
12. GERADIN, M., HOGGE, M., IDELSSOHN, S.: Implicit finite element methods, 417—471 in Belytschko, T., Hughes, T. J. R.: *Computational Methods for Transient Analysis*, Elsevier Science Publishers B. V. (1983).
13. HOLDEN, J. T.: On the finite deflection of thin beams, *Int. J. Solids Struct.*, *8*, 1051—1055 (1972).
14. NAGARAJAN, S., POPOV, E. P.: Elastic-plastic dynamic analysis of axisymmetric solids, *Computers & Structures*, *4*, 1117—1134 (1974).
15. ISHIZAKI, T., BATHE, K. J.: On finite element large displacement and elastic-plastic dynamic analysis of shells structures, *Computers & Structures*, *12*, 309—318 (1980).
16. BATHE, K. J., OZDEMIR, H.: Elastic-plastic large deformation static and dynamic analysis, *Computers & Structures*, *6*, 81—92 (1976).
17. KOVÁCS Á.: Tranzien dynamikus terhelésvizsgálat végeelem módszerrel, *Gép XXXVIII. évf. 6. szám*, 230—233 (1986). (In Hungarian)

Ádám Kovács H-1521, Budapest